PERGAMON

Polyhedron 21 (2002) 2409–2419

POLYHEDRON

www.elsevier.com/locate/poly

Synthesis and structure of platinum and palladium complexes of dimesitylphosphine

Elizabeth M. Pelczar [a], Emily A. Nytko [a], Michael A. Zhuravel [a], Jeremy M. Smith [a,1], David S. Glueck [a,*], Roger Sommer [b], Christopher D. Incarvito [b], Arnold L. Rheingold [b]

[a] 6128 Burke Laboratory, Department of Chemistry, Dartmouth College, Hanover, NH 03755, USA
[b] Department of Chemistry, University of Delaware, Newark, DE 19716, USA

Received 1 May 2002; accepted 31 July 2002

Abstract

Treatment of Pd(tmeda)Me_2 with dimesitylphosphine ($PMes_2H$, L) gave *cis*-PdL_2Me_2 (**1**). *trans*-ML_2Cl_2 (M = Pd (**2**), Pt (**3**)) were prepared from a variety of starting materials. The reaction of Pt(cod)Cl_2 with L gave *cis*-PtL_2Cl_2 (**4**), which reacted with PPh_3 to yield *cis*-Pt(L)(PPh_3)Cl_2 (**5**). *cis*-PtL_2(Me)(Cl) (**6**) was prepared from L and Pt(cod)(Me)(Cl), while reaction of L with Pt(cod)(Et)(I) gave *cis*-PtL_2(Et)(I) (**7**), which isomerized to *trans*-PtL_2(Et)(I) (**8**). The phosphine–borane $PMes_2H{\cdot}BH_3$ (**9**) was made by reaction of L with $BH_3{\cdot}SMe_2$. Crystal structures of **2**·$2CH_2Cl_2$, **4**·CH_2Cl_2, **5**·$2CH_2Cl_2$, **6**, and **9** provided 7information on the steric bulk of L (cone angle ca. 149°). Restricted rotation about the Pt–P and P–C bonds in complexes **4**–**8** was studied by variable temperature NMR spectroscopy.

Keywords: Dimesitylphosphine; Secondary phosphine; X-ray crystallography; NMR; Cone angle; Fluxional

1. Introduction

Since reaction of secondary phosphines with metal complexes often results in cleavage of the P–H bond and formation of a phosphido (PR_2) complex, it is difficult to study their ligand properties for comparison with the well-known tertiary phosphines [1]. Secondary phosphines with bulky substituents are less prone to reactions of the P–H bond, which has enabled extensive study of the coordination chemistry of, for example, P(*t*-Bu)$_2$H [2]. Despite the steric bulk of dimesitylphosphine ($PMes_2H$=L, Mes = 2,4,6-$Me_3C_6H_2$), we have previously reported oxidative addition of its P–H and P–C bonds to Pt(0) [3], as well as cyclometalation of a Mes *o*-Me group in Pt(II) and Pd(II) complexes [4]. Here we describe the synthesis of a series of less reactive Pt(II) and Pd(II) complexes of dimesitylphosphine. NMR and X-ray structural studies provide information on the steric and electronic properties of this ligand, as well as the dynamics of its complexes in solution [5].

2. Results and discussion

Treatment of $PdMe_2$(tmeda) [6] with 2 equiv. of L gave *cis*-Pd($PMes_2H$)$_2Me_2$ (**1**, Scheme 1). The *cis* geometry was established by NMR; thus, the ^{31}P NMR spectrum (C_6D_6) shows only a doublet (J_{PH} = 339 Hz) at δ −46.6, consistent with small $^2J_{PP}$ and $^3J_{PH}$ couplings in the AA′XX′ spin system [7]. The Pd–Me ^{13}C NMR signal (C_6D_6) appears at δ 5.1 (dd, J = 95, 10 Hz), as expected for the *cis* isomer. Tables 1 and 2 contain additional selected NMR and IR (ν_{PH}) data characterizing the $PMes_2H$ ligands in this and related complexes (see below).

Initially prepared samples of **1** were off-white, but they rapidly turned purple in solution or the solid state. Although we were unable to remove the unidentified purple material, these samples were analytically and spectroscopically pure, suggesting that only traces of a

* Corresponding author
E-mail address: glueck@dartmouth.edu (D.S. Glueck).
[1] Department of Chemistry, University of Rochester, Rochester, NY 14627-0216, USA.

0277-5387/02/$ - see front matter
PII: S0277-5387(02)01184-1

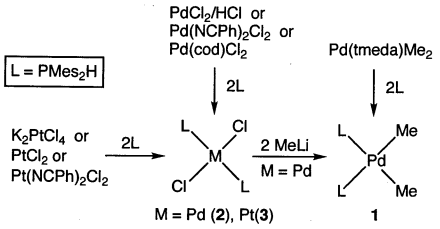

Scheme 1.

highly colored impurity were present. Complex **1** was thermally stable, decomposing slowly in toluene at 105 °C over several days to give unidentified products [8].

Addition of 2 equiv. of $PMes_2H$ to $PdCl_2$ in acidic ethanol gave *trans*-PdL_2Cl_2 (**2**) [9]. This complex could also be prepared by addition of 2 equiv. of $PMes_2H$ to either $Pd(cod)Cl_2$ (cod = 1,5-cyclooctadiene) or $Pd(NCPh)_2Cl_2$ (Scheme 1). The *trans* stereochemistry of **2** and its Pt analogue **3** (see below) was established by NMR. Analysis of the $PMes_2H$ AA′XX′ patterns in the ^1H and ^{31}P NMR spectra [7] and simulation using gNMR [10] gave the coupling constants shown in Table 2. The large J_{PP} values (598 and 523 Hz, respectively) are consistent with the *trans* geometry [11].

Interestingly, treatment of **2** with 2 equiv. of MeLi gave partial conversion to the dimethyl complex **1** (Scheme 1). The steric bulk of $PMes_2H$ would seem to contraindicate the observed *trans*–*cis* isomerization, but similar results have been observed previously. For example, *trans*-$Pd(PPh_3)_2Me_2$ isomerizes on heating in DMSO to the *cis* complex [8a]. Electronic arguments based on the strong *trans* influence of the methyl group

Table 1
Selected NMR and IR data for *cis*-dimesitylphosphine complexes [a]

Complex	δ(P)	$^1J_{PH}$	$^1J_{Pt-P}$	δ(PH)	ν(PH)
PdL_2Me_2 (**1**)	−46.6	339		5.97	2388
PtL_2Cl_2 (**4**) [b]	−48.1	414	3444	6.34	2422
PtL_2Cl_2 (**4A**) [c]	−44.2	408	3631	5.55 [d]	
PtL_2Cl_2 (**4B**) [c]	−51.1	430	3302	6.77 [e]	
PtL_2Cl_2 (**4C**) [c]	−41.6	414	[f]	5.16 [g]	
$PtL(PPh_3)Cl_2$ (**5**) [h]	−39.6 [i]	408	3538	4.89 [j]	2413
$PtL_2(Me)(Cl)$ (**6**)	−38.1	372	1505	[f]	2400
	−49.2	403	4189		
$PtL_2(Me)(Cl)$ (**6A**) [k]	−31.8	[m]	1777	[m]	
	−47.3		3996		
$PtL_2(Me)(Cl)$ (**6B**) [k]	−33.7	[m]	1726	[m]	
	−48.1		4016		
$PtL_2(Me)(Cl)$ (**6C**) [k]	−34.9	[m]	1341	[m]	
	−43.2		4207		
$PtL_2(Me)(Cl)$ (**6D**) [k]	−36.4	[m]	1444	[m]	
	−44.1		4234		
$PtL_2(Et)(I)$ (**7**)	−43.5	388	4315	[f]	2402
	−46.9	368	1350		
$PtL_2(Et)(I)$ (**7A**) [l]	−41.7	386	4355	[m]	
	−46.3	382	1325		
$PtL_2(Et)(I)$ (**7B**) [l]	−40.1	401	4309	[m]	
	−44.0	375	1248		
$PtL_2(Et)(I)$ (**7C**) [l]	−37.1	389	4166	[m]	
	−41.2	361	1627		
$PtL_2(Et)(I)$ (**7D**) [l]	−35.8	409	4132		
	−39.4	362	1563	[m]	

[a] Temperature: 21 °C unless noted; solvents: C_6D_6 for **1**, **6**, $CDCl_3$ for **5**, **7**. ^{31}P NMR chemical shift reference: external 85% H_3PO_4; coupling constants in Hz; IR data in cm^{-1} for KBr pellets.
[b] C_6D_5Cl, 100 °C.
[c] CD_2Cl_2, −70 °C. Two major species (A, B) and a minor one (C) in ca. 1:1:0.15 ratio were observed.
[d] Apparent dd, $J = 408$, 10.
[e] Apparent d, $J = 430$.
[f] Not observed.
[g] Apparent dd, $J = 414$, 10. In addition, another apparent d ($J = 428$) at δ 6.89 was observed.
[h] Additional ^{31}P NMR data: δ 14.5 (d, $J = 14$, $J_{Pt-P} = 3589$, PPh_3).
[i] d, $J = 14$.
[j] dd, $J = 408$, 12.
[k] CD_2Cl_2, −70 °C. Four isomers A–D (ratio 2.9:2.6:1.7:1) were observed; for isomers B–D, $J_{PP} = 8$.
[l] CD_2Cl_2, −40 °C. Four isomers A–D (ratio 7.3:4.4:5.6:1) were observed.
[m] See the text and Section 4 for further discussion and low-temperature ^1H NMR results.

Table 2
Selected NMR and IR data for *trans*-dimesitylphosphine complexes [a]

Complex	δ(P)	$^1J_{Pt-P}$	$^2J_{PP}$	$^1J_{PH}$	$^3J_{PH}$	δ(PH)	ν(PH)
PdL_2Cl_2 (**2**)	−38.3		598	386	−2	6.52	2400
PtL_2Cl_2 (**3**)	−37.9	2506	523	396	−2	6.66	2404
$PtL_2(Et)(I)$ (**8**) [b,c]	−37.1	3123	492	389	−3	7.24 [d]	2395

[a] Temperature: 21 °C unless noted; solvents: $CDCl_3$ for **2**, **3**, C_6D_5Cl for **8**; ^{31}P NMR chemical shift reference: external 85% H_3PO_4; coupling constants in Hz; IR data in cm^{-1} for KBr pellets.
[b] 80 °C.
[c] Additional $^{31}P\{^1H\}$ NMR data for **8** (CD_2Cl_2, −70 °C): Four isomers (A–D) with approximate ratio 4.8:2.7:1:1 were observed; δ −39.4 (J_{Pt-P} = 3069, A), −29.0 (J_{Pt-P} = 3153, B), −37.3 (J_{Pt-P} = 3006, C), −26.7 (J_{Pt-P} = 3153, D). See the text and Section 4 for additional discussion of these and related low-temperature ^1H NMR spectra.
[d] Apparent d, J = 384, J_{Pt-H} = 26, perhaps the most intense two peaks of an AA′XX′ pattern.

have been advanced to explain this behavior (''anti-symbiotic effect'' [12], ''transphobia'' [13]).

Reaction of 2 equiv. of L with three different platinum sources [K_2PtCl_4, $PtCl_2$, and $PtCl_2(NCPh)_2$] yielded *trans*-$Pt(PMes_2H)_2Cl_2$ (**3**) as a yellow powder (Scheme 1, Table 2). In contrast, treatment of $Pt(cod)Cl_2$ with L gave *cis*-$Pt(PMes_2H)_2Cl_2$ (**4**) as shown in Scheme 2. Its room temperature NMR spectra contain very broad peaks, attributed to restricted rotation about the P–C and/or Pt–P bonds (see below). At high temperature (100 °C, C_6D_5Cl) a sharp average spectrum consistent with the *cis* geometry is observed (Table 1).

The reactivity of **4** was briefly examined (Scheme 2). Irradiation of a CD_2Cl_2 solution of **4** with a mercury lamp caused slow conversion to the *trans* isomer **3**, consistent with literature reports of related photochemical *cis*–*trans* isomerizations in PtL_2X_2 complexes (L = PPh_3, pyridine, isoquinoline, X = Cl, Br) [9,14]. Treatment of $Pt(cod)Cl_2$ with 3 equiv. of $PMes_2H$ gave a mixture of **4** and $PMes_2H$, which did not undergo exchange on the NMR time scale, while 1 equiv. of $PMes_2H$ gave a mixture of **4** and unreacted $Pt(cod)Cl_2$, as shown by the ^1H NMR spectrum. Addition of more phosphine completed the conversion to **4**. $PMes_2H$ was readily displaced from **4** by 2 equiv. of dppe (dppe = $Ph_2PCH_2CH_2PPh_2$) to yield $[Pt(dppe)_2][Cl]_2$ [15]. Heating **4** at 45 °C in CH_2Cl_2 with 2 equiv. of PPh_3 gave *cis*-$Pt(PMes_2H)(PPh_3)Cl_2$ (**5**). Consistent with the stoichiometry, ^{31}P NMR monitoring of the reaction mixture showed formation of $PMes_2H$ and the presence of unreacted PPh_3. Recrystallization from CH_2Cl_2/petroleum ether gave white crystals, identified by NMR as the *cis* isomer (J_{PP} = 14 Hz, Table 1).

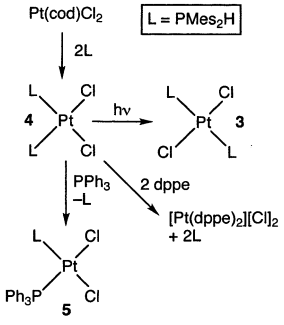

Scheme 2.

Reaction of Pt(cod)(Me)(Cl) with 2 equiv. of L yielded *cis*-$Pt(PMes_2H)_2(Me)(Cl)$ (**6**, Scheme 3). The *cis* geometry was established by ^{31}P NMR (see Table 1) and by the Pt–Me ^{13}C NMR signal (δ 3.5, dd, J = 96, 6 Hz, CD_2Cl_2). Similarly, treatment of Pt(cod)(Et)(I) with 2 equiv. of L gave white *cis*-$Pt(PMes_2H)_2(Et)(I)$ (**7**, Table 1), which readily isomerized on standing or gentle heating to the yellow *trans* isomer (**8**, Scheme 3). The room temperature NMR spectra of complex **8** were very broad, indicative of a dynamic process (see Section 2.2), but at 80 °C in C_6D_5Cl, it showed the expected AA′XX′ ^{31}P NMR spectrum (Table 2).

2.1. Solid-state structures

The X-ray crystal structures of *trans*-PdL_2Cl_2 (**2**·$2CH_2Cl_2$), *cis*-PtL_2Cl_2 (**4**·CH_2Cl_2), *cis*-$PtL(PPh_3)Cl_2$ (**5**·$2CH_2Cl_2$), *cis*-$PtL_2(Me)(Cl)$ (**6**) and the phosphine–borane L-BH_3 (**9**, see Section 4) were determined to investigate the effect of the bulky phosphine on the structures of its simple coordination complexes. For thermal ellipsoid plots, see Figs. 1–5; crystal data is summarized in Table 3, and additional details are included in Sections 4 and 5. See the figure captions and Tables 4 and 5 for selected bond lengths and angles.

The structure of **2** shows a minor distortion from ideal square planar geometry, and Pd–P and Pd–Cl bond

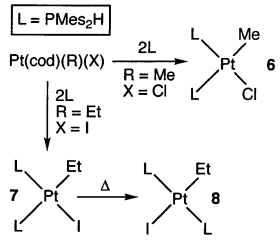

Scheme 3.

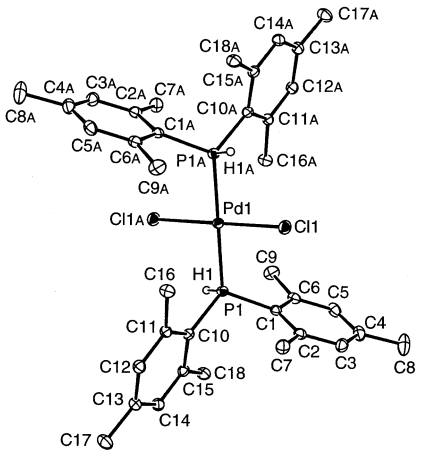

Fig. 1. ORTEP diagram of *trans*-$Pd(PMes_2H)_2Cl_2$ (**2**·$2CH_2Cl_2$), with thermal ellipsoids at 30% probability. The solvent molecules and hydrogen atoms, except those on P, have been removed for clarity. Selected bond lengths (Å) and angles (°): Pd–Cl(1) 2.3028(7), Pd–Cl(1A) 2.3028(7), Pd–P(1) 2.3057(7), Pd–P(1A) 2.3057(7), P(1)–C(10) 1.819(3), P(1)–C(1) 1.822(3), Cl(1)–Pd–Cl(1A) 180.0, Cl(1)–Pd–P(1) 93.91(2), Cl(1A)–Pd–P(1) 86.09(2), Cl(1)–Pd–P(1A) 86.09(2), Cl(1)–Pd–P(1) 93.91(2), P(1)–Pd–P(1A) 180.0, C(10)–P(1A)–C(1) 110.45(12).

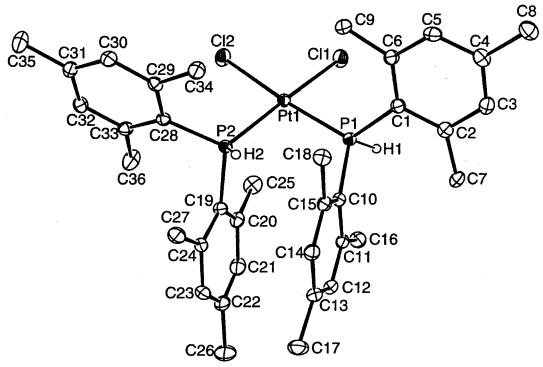

Fig. 2. ORTEP diagram of *cis*-$Pt(PMes_2H)_2Cl_2$ (**4**·CH_2Cl_2), with thermal ellipsoids at 30% probability. The solvent molecule and hydrogen atoms, except those on P, have been removed for clarity.

lengths typical of those in square planar phosphine complexes [16]. The *cis*-Pt complexes **4**–**6** (see Table 4) all show slight distortions from square planar geometry. As might be expected, the P–Pt–P bond angles, which range from 95.65(7)° to 97.07(7)° are larger than the ideal value, presumably due to steric hindrance between the bulky phosphines, as previously observed in *cis*-$Pt(PPh_3)_2Cl_2$ (Table 4) and related structures [17]. The close similarity between the structures of **4**, **5** and *cis*-$Pt(PPh_3)_2Cl_2$ suggests that L and PPh_3 have comparable steric and electronic properties. This is consistent with the similar J_{Pt-P} values found for these phosphines in **5** (3538 Hz for L, 3589 Hz for PPh_3, $CDCl_3$). As expected from *trans* influence trends, the Pt–P bond *trans* to the methyl group in **6** is longer [2.3311(17) Å] than the one *trans* to chloride [2.214(2) Å] [18].

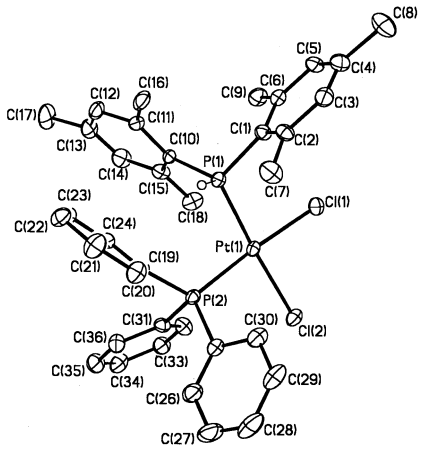

Fig. 3. Thermal ellipsoid plot (25% probability) of *cis*-$Pt(PMes_2H)(PPh_3)Cl_2$ (**5**·$2CH_2Cl_2$). The solvent molecule and hydrogen atoms, except the one on P, have been removed for clarity.

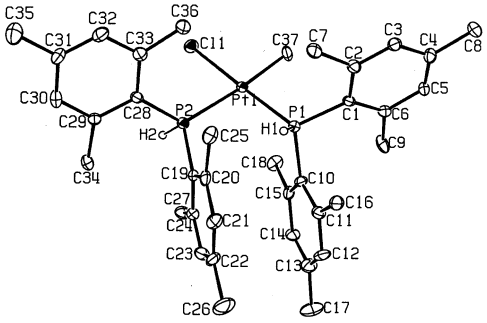

Fig. 4. ORTEP diagram of *cis*-$Pt(PMes_2H)_2(Me)(Cl)$ (**6**), with thermal ellipsoids at 30% probability. The hydrogen atoms, except those on P, have been removed for clarity.

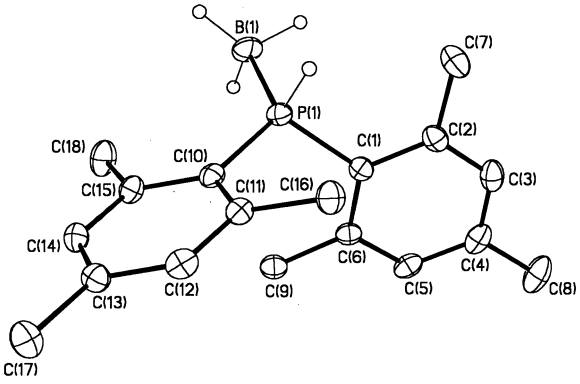

Fig. 5. Thermal ellipsoid plot (25% probability) of $PMes_2H{\cdot}BH_3$ (**9**). Hydrogen atoms, except those on P and B, have been removed for clarity. Selected bond lengths (Å) and angles (°): P–H(1) 1.35(3), P–C(1) 1.824(3), P–C(10) 1.829(3), P–B(1) 1.938(4), H(1)–P–C(10) 97.3(11), H(1)–P–C(1) 104.0(11), H(1)–P–B(1) 108.3(12), C(10)–P–C(1) 110.71(12), C(10)–P–B(1) 124.41(15), C(1)–P–B(1) 109.62(15).

In the structure of phosphine–borane **9**, the PH and BH_3 hydrogens were found and refined freely. The geometry around phosphorus is tetrahedral as expected, though the C(10)–P–B bond angle is somewhat larger

Table 3
Crystallographic data for *trans*-PdL_2Cl_2 (**2**·$2CH_2Cl_2$), *cis*-PtL_2Cl_2 (**4**·CH_2Cl_2), *cis*-$PtL(PPh_3)Cl_2$ (**5**·$2CH_2Cl_2$), *cis*-$PtL_2(Me)(Cl)$ (**6**), and L·BH_3 (**9**)

Complex	**2**·$2CH_2Cl_2$	**4**·CH_2Cl_2	**5**·$2CH_2Cl_2$	**6**	**9**
Empirical formula	$C_{38}H_{50}Cl_6P_2Pd$	$C_{37}H_{48}Cl_4P_2Pt$	$C_{38}H_{42}Cl_6P_2Pt$	$C_{37}H_{49}ClP_2Pt$	$C_{18}H_{26}BP$
Formula weight	887.82	891.58	968.45	786.24	284.17
Space group	$P2_1/n$	$P2_1/n$	$P2_1/n$	$P2_1/n$	$P2_1/c$
Temperature (K)	173(2)	173(2)	173(2)	173(2)	173(2)
a (Å)	11.3321(6)	12.4534(10)	11.6372(13)	14.2510(9)	8.1454(14)
b (Å)	11.8745(7)	19.3221(15)	22.830(3)	15.1847(11)	11.3460(19)
c (Å)	15.9474(8)	16.1326(12)	15.2546(18)	16.2727(11)	19.258(3)
α (°)	90	90	90	90	90
β (°)	107.6950(10)	106.418(2)	98.820(3)	97.257(2)	98.973(4)
γ (°)	90	90	90	90	90
V (Å^3)	2044.40(19)	3723.6(5)	4004.9(8)	3493.2(4)	1758.0(5)
Z	2	4	4	4	4
λ (Å)	0.71073	0.71073	0.71073	0.71073	0.71073
D_{calc} (g cm^{-3})	1.442	1.590	1.606	1.495	1.074
μ (mm^{-1})	0.951	4.167	4.010	4.209	0.146
$R(F)$ (%) [a]	3.59	2.98	4.02	4.79	5.53
$R(wF^2)$ (%) [a]	8.44	6.52	8.91	7.87	13.50

[a] Quantity minimized = $R(wF^2) = [\Sigma[w(F_o^2 - F_c^2)^2]/\Sigma[w(F_o^2)^2]]^{1/2}$; $R = \Sigma\Delta/\Sigma(F_o)$, $\Delta = I|(F_o - F_c)|I$.

than the ideal angle at 124.41(15)°. The P–B bond length (1.938(4) Å) is typical of those in phosphine–boranes, for which a recently reported range is 1.832–1.983 Å [19]. Comparison to the structure of $PMes_2H$ [20] (Table 5) shows that borane complexation has little effect on the structure of the phosphine. The P–C bonds become slightly shorter and the C(1)–P–C(10) bond angle is increased.

The program STERIC [21] was used to determine the cone angle of L from the crystal structure data, setting a P–B distance of 2.28 Å in the case of **9** [22]. Although this is longer than the experimental distance, this choice allows comparison to the results for the metal complexes. As shown in Table 6, the cone angle falls in a narrow range in this series of complexes, although significant differences can be seen even within a single compound containing two phosphines, such as **4**. The average cone angle is approximately 149°. Consistent with the discussion above, the crystallographically determined cone angles for L and PPh_3 in **5** are similar;

Table 4
Selected bond lengths (Å) and angles (°) for *cis*-Pt dimesitylphosphine complexes **4**–**6** [a]

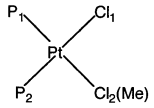

Complex	PtL_2Cl_2 (**4**·CH_2Cl_2)	$PtL(PPh_3)Cl_2$ (**5**·$2CH_2Cl_2$)	$PtL_2(Me)(Cl)$ (**6**)	$Pt(PPh_3)_2Cl_2·C_3H_6O$ [b]
Bond lengths				
Pt–P_1	2.2481(9)	2.2438(19)	2.3311(17)	2.251(2)
Pt–P_2	2.2315(9)	2.2444(19)	2.214(2)	2.265(2)
Pt–Cl_1	2.3445(10)	2.3519(19)	2.3591(19)	2.333(2)
Pt–Cl_2 (Me)	2.3385(9)	2.3478(19)	2.084(6)	2.356(2)
Bond angles				
P_1–Pt–P_2	96.93(3)	95.65(7)	97.07(7)	97.8(1)
P_1–Pt–Cl_1	84.13(3)	89.63(7)	85.29(7)	89.8(1)
P_1–Pt–Cl_2 (Me)	173.90(3)	175.02(6)	172.0(2)	176.9(1)
Cl_1–Pt–Cl_2 (Me)	89.79(4)	88.15(7)	87.3(2)	87.1(1)
Cl_1–Pt–P_2	174.46(4)	174.61(6)	177.19(7)	172.4(1)
P_2–Pt–Cl_2 (Me)	89.10(3)	86.68(7)	90.3(2)	85.3(1)

[a] For **4**·CH_2Cl_2, $P_1 = P_2 = L$; for **5**·$2CH_2Cl_2$, $P_1 = L$, $P_2 = PPh_3$; for **6**, $P_1 = P_2 = L$, P_1 *trans* to Me, P_2 *trans* to Cl. Note that the atom numbering in Fig. 5 for **6** is slightly different than the convention used here.
[b] Ref. [17].

Table 5
Selected bond lengths (Å) and angles (°) in $PMes_2H$ [a] and $PMes_2H \cdot BH_3$ (**9**)

Complex	$PMes_2H$	$PMes_2H \cdot BH_3$ (**9**)
Bond lengths		
P–C(1)	1.862(7)	1.824(3)
P–C(10)	1.864(7)	1.829(3)
P–H(1)	1.36(7)	1.35(3)
Bond angles		
C(1)–P–C(10)	107.0(3)	110.71(12)
C(1)–P–H(1)	109(3)	104.0(11)
C(10)–P–H(1)	107(3)	97.3(11)

[a] Ref. [20].

Table 6
Cone angle data for dimesitylphosphine complexes [a]

Complex	Cone angle (°)
trans-PdL_2Cl_2 (**2**·$2CH_2Cl_2$)	147
cis-PtL_2Cl_2 (**4**·CH_2Cl_2)	152, 142
cis-$PtL(PPh_3)Cl_2$ (**5**·$2CH_2Cl_2$)	148 [b]
cis-$PtL_2(Me)(Cl)$ (**6**)	156, 154
$L \cdot BH_3$ (**9**)	146
cis-$Pt(PPh_3)_2Cl_2 \cdot C_3H_6O$ [c]	143, 150

[a] See Section 4 for details of the calculations.
[b] PPh_3 cone angle = 154°.
[c] Ref. [17].

compare to Tolman's reported cone angle of 145° for PPh_3 [22].

2.2. Solution structures: fluxional processes

Conformational isomerism due to restricted rotation has often been observed in metal complexes of bulky secondary phosphines. For example, Shaw reported that room-temperature solutions of *trans*-$Pt[P(t\text{-}Bu)_2H]_2Cl_2$ contained two conformational isomers; this complex has recently been studied in more detail by Mastrorilli et al. [23]. Similarly, Bushweller's detailed investigation of *trans*-$Rh[P(t\text{-}Bu)_2H]_2(CO)(X)$ (X = halide) revealed several conformations as a result of restricted rotation about the Rh–P bonds [24], and analogous behavior was observed for $Ir[P(t\text{-}Bu)_2H]_3(Cl)$ [2c]. We observed similar phenomena in Pt dimesitylphosphine complexes **4**–**8** by low-temperature NMR spectroscopy.

Although the room-temperature ^{31}P NMR spectrum of *cis*-PtL_2Cl_2 (**4**) was very broad, three different signals in about a 1:1:0.15 ratio were observed at −70 °C in CD_2Cl_2 (Table 1). We assign these to two major isomers (A and B) and one minor one (C), although we cannot rule out the possibility that the A and B signals are in fact due to a single conformer which contains two inequivalent dimesitylphosphine ligands [24].

Low-temperature ^1H NMR studies (−70 °C, CD_2Cl_2) provided additional information on the dynamic processes in **4**. As detailed in Section 4, 12 aryl proton signals (8 from the major and 4 from the minor isomers) and 18 methyl signals (12 major, 6 minor) were observed. These observations can be explained if, in the two major isomers, rotation about the P–C and Pt–P bonds is slow on the NMR time scale. If rotation about the P–C bond is slow, the *o*-Me and *m*-aryl protons are inequivalent in a given Mes group; if rotation about the Pt–P bond is slow, then there are two types of mesityl groups in a given $PMes_2H$. The crystal structure (Fig. 2), if maintained in solution at low temperature, would be consistent with these observations. The two major isomers might then be *syn* and *anti* conformers, as reported for *trans*-$Pt[P(t\text{-}Bu)_2H]_2Cl_2$ [23].

Four P–H resonances were also observed (Table 1). Three of these are easily assigned, one each to the major and minor isomers, from matching the P–H couplings in the low temperature ^1H NMR spectrum with those obtained in the low temperature ^{31}P NMR spectrum, but the origin of the fourth signal is not clear. These P–H resonances are expected to show an AA′XX′ pattern, but either simple doublets or doublet of doublets patterns were observed. If the $^2J_{PP}$ and $^3J_{PH}$ couplings are small, then the signals would appear as a doublet. The doublet of doublets patterns could arise if $^2J_{PP}$ is small. Alternatively, the observed resonances could be due to the inner lines of an AA′XX′ pattern, if the low intensity outer peaks are not observed [7].

Similarly, at −20 °C in CD_2Cl_2, the rotation about the P–C and Pt–P bonds in **5** is slow on the NMR time scale, so each of the Mes *m*-aryl protons and *o*-Me groups is inequivalent, consistent with the conformation found in the crystal structure (Fig. 3). Thus, four sharp peaks for the Mes *m*-aryl protons were observed from 6.92 to 6.63 ppm, and four *o*-Me signals appeared at δ 3.38, 2.50, 1.85, and 1.20. Because the two Mes groups are inequivalent, two separate *p*-Me resonances were observed at δ 2.25 and 2.23.

The related complexes **6** and **7** showed similar fluxional behavior, again ascribed to restricted rotation about the Pt–P and P–C bonds, giving rise to four different isomers in each case at low temperature. This could be observed most clearly by ^{31}P NMR (Table 1). Five and six of the expected eight P–H resonances could also be observed by low-temperature ^1H NMR for **6** and **7**, respectively (see Section 4 for details).

trans-$PtL_2(Et)(I)$ (**8**) also showed broad peaks in the room temperature NMR spectra. As for the *cis* isomer **7**, four isomers were observed by low-temperature ^{31}P NMR (Table 2). However, the lines in the expected AA′XX′ patterns could not all be resolved because of weak, overlapping signals. Similarly, the ^1H NMR spectrum (CD_2Cl_2, −70 °C) revealed the most intense

signals of the four expected PH AA′XX′ patterns; however, two of these peaks were obscured by Mes resonances (see Table 2 and Section 4).

3. Conclusion

We prepared several simple coordination complexes of the bulky secondary phosphine $PMes_2H$. Its crystallographically determined cone angle of approximately 149° is comparable to that of PPh_3, and comparison of the structures of *cis*-PtL_2Cl_2 (**4**), *cis*-$PtL(PPh_3)Cl_2$ (**5**), and *cis*-$Pt(PPh_3)_2Cl_2$ shows these ligands to have similar steric and electronic properties. The bulk of dimesitylphosphine is reflected in the dynamic properties of its complexes in solution at low temperature, where restricted rotation about Pt–P and P–C(Mes) bonds was frequently observed.

4. Experimental

4.1. General

Unless otherwise noted, all reactions and manipulations were performed in dry glassware under a nitrogen atmosphere at 20 °C in a dry box or using standard Schlenk techniques. Petroleum ether (b.p. 38–53 °C), ether, THF, CH_2Cl_2 and toluene were dried and degassed using columns with activated alumina [25].

NMR spectra were recorded (at 21 °C unless otherwise noted) with Varian 300 or 500 MHz spectrometers; the latter was used for variable temperature studies. ^1H or ^{13}C NMR chemical shifts are reported versus Me_4Si and were determined by reference to the residual ^1H or ^{13}C solvent peaks. ^{31}P NMR chemical shifts are reported versus H_3PO_4 (85%) used as an external reference. Coupling constants are reported in Hz, as absolute values unless noted otherwise. Unless indicated, peaks in NMR spectra are singlets. Infrared spectra were recorded using KBr pellets on a Perkin Elmer 1600 series FTIR machine and are reported in cm^{-1}. Elemental analyses were provided by Schwarzkopf Microanalytical Laboratory. Low resolution FAB Mass Spectroscopy was performed on a VG ZAB-SE instrument at the University of Illinois.

Unless otherwise noted, reagents were from commercial suppliers. The following compounds were made by the literature methods: $Pd(tmeda)Me_2$ [6], $PMes_2H$ [20], $Pd(cod)Cl_2$ [26], $Pd(NCPh)_2Cl_2$ [27], $Pt(NCPh)_2Cl_2$ [27], $Pt(cod)Cl_2$ [28], Pt(cod)(Me)(Cl) [29], and Pt(cod)(Et)(I) [30].

4.2. *cis*-$Pd(PMes_2H)_2Me_2$ (**1**). Method 1

$Pd(tmeda)Me_2$ (80 mg, 0.32 mmol) and $PMes_2H$ (165 mg, 0.610 mmol) were dissolved in 10 ml of THF to give a pink–red solution. The THF was removed under vacuum to give a brownish white solid, which was washed with petroleum ether (4 ml). The resulting blood-red solution was removed using a pipet to give a pink solid, which was dried under vacuum to yield 189 mg (88%) of the product.

Anal. Calc. for $C_{44}H_{52}P_2Pd$: C, 67.40; H, 7.74. Found: C, 67.23; H, 7.32%. ^1H NMR (C_6D_6): δ 6.55 (8H, Mes), 5.97 (d, $J_{PH} = 339$, 2H, PH), 2.33 (broad, 24H, *o*-Me), 2.01 (12H, *p*-Me), 1.00 (m, 6H, Pd–Me). $^{13}C\{^1H\}$ NMR (C_6D_6): δ 142.7 (Mes), 139.1 (Mes), 130.2 (t, $J = 3$, Mes), 126.3 (d, $J = 26$, Mes), 23.7 (Me), 21.2 (Me), 5.0 (dd, $J = 105$, 10, Pd–Me). IR: 3433, 2922, 2388, 1727, 1600, 1450, 1377, 1133, 1027, 844, 694, 616, 550.

4.3. Method 2

A pale yellow solution of *trans*-$Pd(PMes_2H)_2Cl_2$ (26 mg, 3.6×10^{-2} mmol, **2**, see below) in 10 ml of THF was cooled to −78 °C and treated with methyllithium (106 μl of 1.4 M solution in ether, 0.15 mmol). The resulting golden solution was stirred for 1 h at −78 °C, then quenched by the addition of one drop of water, which turned the solution orange. The solution was concentrated under vacuum and transferred to a NMR tube. The ^{31}P NMR spectrum showed partial conversion (73%) of the dichloro complex **2** to the dimethyl complex **1**. ^{31}P NMR (THF/ether): δ −34.8 (AA′XX′, **2**), −48.3 (d, $J = 339$, **1**).

4.4. *trans*-$Pd(PMes_2H)_2Cl_2$ (**2**). Method 1

$PdCl_2$ (57 mg, 0.32 mmol) was treated with concentrated HCl (4 ml) and the brown solution was stirred for 10 min. After addition of 8 ml of absolute ethanol, the solution was stirred for an additional 5 min. A solution of $PMes_2H$ (174 mg, 0.643 mmol) in 4 ml of ether was added, causing a yellow precipitate to form immediately. The mixture was allowed to stir for another 5 min, and then filtered on a frit. The solid was washed with water (1×10 ml) and ether (2×20 ml) and dried on the frit to give 230 mg, 99%. The yellow solid was recrystallized from methylene chloride/petroleum ether to give yellow crystals of a methylene chloride solvate, as quantified by ^1H NMR integration.

Anal. Calc. for $C_{36}H_{46}Cl_2P_2Pd \cdot 0.6CH_2Cl_2$: C, 57.17; H, 6.19. Found: C, 57.06; H, 6.12%. ^1H NMR ($CDCl_3$): δ 6.85 (8H, Mes), 6.52 (m, $J_{PP} = 598$, $J_{PH} = 386$, $J_{PH'} = -2$, 2H, P–H, AA′XX′), 2.52 (24H, *o*-Me), 2.25 (12H, *p*-Me). $^{13}C\{^1H\}$ NMR ($CDCl_3$, 21 °C): δ 142.5 (t, $J = 5$, Mes), 140.9 (Mes), 130.1 (t, $J = 4$, Mes), 122.1 (t, $J = 24$,

Mes), 23.7 (t, $J = 4$, *o*-Me), 21.3 (*p*-Me). IR: 2956, 2922, 2400, 1600, 1556, 1449, 1405, 1374, 1264, 1029, 837.

4.5. Method 2

A yellow solution of $Pd(cod)Cl_2$ (22 mg, 0.11 mmol) in methylene chloride was treated with $PMes_2H$ (86 mg, 0.32 mmol), causing the solution to turn orange. ^{31}P NMR (CH_2Cl_2): δ −41.0 (AA′XX′, $J_{PP} = 597$, $J_{PH} = 386$, $J_{PH'} = -0.07$). Recrystallization from methylene chloride and petroleum ether gave yellow crystals of compound **2**.

4.6. Method 3

A brown slurry of $Pd(NCPh)_2Cl_2$ (22 mg, 5.7×10^{-2} mmol) in 10 ml of CH_2Cl_2 was treated with $PMes_2H$ (46.5 mg, 0.173 mmol), which gave a homogeneous yellow solution. $^{31}P\{^1H\}$ NMR (CH_2Cl_2): δ −41.0.

4.7. *trans*-$Pt(PMes_2H)_2Cl_2$ (**3**). Method 1

$PMes_2H$ (50 mg, 0.19 mmol) was dissolved in 10 ml of ethanol with gentle heating, then cooled to room temperature. A red–orange solution of K_2PtCl_4 (38 mg, 9.1×10^{-2} mmol) in 14 ml of water was added to the phosphine solution, and a fine white precipitate immediately formed. The mixture was filtered through a fine frit, and the solid was air dried to give 38 mg (51%) of the product as a very fine white powder. Recrystallization from methylene chloride/petroleum ether gave yellow crystals of a methylene chloride solvate. These crystals desolvated under vacuum to give an analytically pure sample.

Anal. Calc. for $C_{36}H_{46}Cl_2P_2Pt$: C, 53.60; H, 5.75. Found: C, 53.58; H, 5.91%. ^1H NMR ($CDCl_3$): δ 6.85 (8H, Mes), 6.66 (m, $J_{PP} = 523$, $J_{PH} = 396$, $J_{P'H} = -2$, 2H, P-H, AA′XX′), 2.53 (24H, *o*-Me), 2.25 (12H, *p*-Me). $^{13}C\{^1H\}$ NMR ($CDCl_3$): δ 142.6 (t, $J = 6$, Mes), 140.7 (Mes), 130.2 (t, $J = 4$, Mes), 121.5 (t, $J = 28$, Mes), 23.5 (t, $J = 4$, *o*-Me), 21.3 (*p*-Me). IR: 2956, 2731, 2404, 1599, 1559, 1446, 1407, 1373, 1289, 1243, 1029, 962, 933, 905, 849, 708, 623, 550, 420.

4.8. Method 2

A CH_2Cl_2 solution of $PtCl_2(NCPh)_2$ (10 mg, 2.2×10^{-2} mmol) was treated with $PMes_2H$ (15 mg, 4.2×10^{-2} mmol). The $^{31}P\{^1H\}$ NMR spectrum of the reaction mixture showed that **3** had formed: δ −37.9 ($J_{Pt-P} = 2506$).

4.9. Method 3

A NMR tube containing a clear solution of *cis*-$PtCl_2(PMes_2H)_2$ (**4**) (20 mg, 2.5×10^{-2} mmol, **4**, see below) in 1 ml of CH_2Cl_2 was suspended about 3 cm from an Ace-Hanovia Photochemical Lamp with a mercury bulb. The tube was irradiated and monitored by $^{31}P\{^1H\}$ NMR. After 9 h the solution was pale yellow and the ^{31}P NMR spectrum showed about 10% conversion of **4** to **3**.

4.10. *cis*-$PtCl_2(PMes_2H)_2$ (**4**)

A solution of $Pt(cod)Cl_2$ (100 mg, 0.267 mmol) in CH_2Cl_2 (4 ml) was treated with $PMes_2H$ (145 mg, 0.535 mmol). Petroleum ether (10 ml) was layered on the methylene chloride and the clear solution was cooled to −20 °C, yielding white crystals after several days. The mother liquor was removed and the crystals dried under vacuum to give 151 mg (70%) of product. ^1H NMR integration and elemental analysis showed that these crystals contained CH_2Cl_2.

Anal. Calc. for $C_{36}H_{46}Cl_2P_2Pt \cdot 0.8CH_2Cl_2$: C, 50.54; H, 5.49. Found: C, 50.12; H, 5.25%. $^{31}P\{^1H\}$ NMR (CD_2Cl_2, 21 °C): δ −47.5 (very broad, $J_{Pt-P} = 3508$). ^1H NMR (CD_2Cl_2, 21 °C): δ 6.78 (broad), 2.39 (very broad), 2.26 (broad). $^{13}C\{^1H\}$ NMR (CD_2Cl_2, 21 °C): δ 142.5 (broad), 141.7, 130.6, 23.7 (broad), 21.1. IR: 3444, 2955, 2911, 2722, 2422, 1600, 1555, 1444, 1405, 1377, 1288, 1255, 1027, 950, 900, 877, 850, 727, 616, 550, 444. FAB mass spectrum (Magic Bullet): *m*/*z* 870, 734 $(PtPMes_2H)(PMes_2)^+$), 600, 463, 343, 271 ($PMes_2H$), 234, 135, 119 (Mes).

^1H NMR (CD_2Cl_2, −70 °C): Three isomers A–C were observed; unless otherwise noted, the ^1H NMR signals are assigned to A and B, with specific assignments given where possible. δ 7.02 (C), 6.98 (d, $J = 3$, 2H, Mes), 6.94 (2H, Mes), 6.91 (C), 6.89 (d, $J = 428$, PH, C), 6.88 (d, $J = 3$, 2H, Mes), 6.86 (C), 6.82 (2H, Mes), 6.78 (C), 6.77 (d, $J = 430$, 2H, PH, B), 6.73 (2H, Mes), 6.68 (2H, Mes), 6.52 (2H, Mes), 6.48 (C), 6.11 (2H, Mes), 5.55 (apparent dd, $J = 408$, 10, 2H, PH, A), 5.16 (apparent dd, $J = 414$, 10, PH, C), 3.41 (6H), 3.37 (6H), 3.33 (C), 3.20 (C), 2.65 (6H), 2.42 (C), 2.26 (6H), 2.23 (6H), 2.22 (6H), 2.08 (6H), 2.07 (6H), 2.03 (C), 1.99 (6H), 1.98 (6H), 1.89 (6H), 1.39 (6H), 1.20 (C), 0.90 (C). $^{13}C\{^1H\}$ NMR (CD_2Cl_2, −60 °C): δ 143.9 (d, $J = 15$), 143.4 (d, $J = 14$), 143.0 (d, $J = 8$), 142.0 (m), 141.5 (m), 141.3 (d, $J = 6$), 141.1 (m), 140.9 (m), 139.9 (m), 139.7 (m), 139.4 (m), 131.0–130.8 (m), 130.3 (d, $J = 10$), 129.7 (m), 129.4 (d, $J = 8$), 129.2 (m), 121.7, 121.2, 118.2, 118.0, 117.9, 117.4, 117.1, 116.7 (m), 27.1 (d, $J = 9$), 26.4 (d, $J = 10$), 22.6–22.2 (m), 21.7 (m), 20.9–20.5 (m).

^1H NMR (C_6D_5Cl, 21 °C): δ 6.53 (broad, Mes), 2.31 (broad, *o*-Me), 2.05 (*p*-Me). ^1H NMR (C_6D_5Cl, 100 °C): δ 6.57 (8H, Mes), 6.34 (d, $J = 414$, 2H, PH), 2.38 (24H, *o*-Me), 2.06 (12H, *p*-Me). $^{31}P\{^1H\}$ NMR (C_6D_5Cl, 21 °C): δ −48.7 (very broad).

4.11. *cis*-Pt(PMes$_2$H)(PPh$_3$)Cl$_2$ (**5**)

PPh_3 (49 mg, 0.19 mmol) was dissolved in methylene chloride (6 ml) to give a clear solution. *cis*-$PtCl_2(PMes_2H)_2$ (100 mg, 0.124 mmol) was added. No color change occurred, and the solid did not dissolve completely. The solution was filtered through Celite to give a yellow filtrate. After the solution was left standing at room temperature overnight, it turned clear. The solution was heated to 45 °C for 5 h using a water bath. The solvent was then removed under vacuum to give white crystals, which were recrystallized from methylene chloride/petroleum ether to give 51 mg (52%) of white solid which was a CH_2Cl_2 solvate, according to the ^{1}H NMR spectrum in $CDCl_3$. Recrystallization from THF/ether gave analytically pure material.

Anal. Calc. for $C_{36}H_{38}Cl_2P_2Pt$: C, 54.14; H, 4.80. Found: C, 54.45; H, 4.60%. ^{1}H NMR (CD_2Cl_2, 21 °C): δ 7.66–7.62 (m, 6H, Ph), 7.47 (m, 3H, Ph), 7.36–7.32 (m, 6H, Ph), 6.89–6.62 (broad, 4H, Mes), 4.89 (dd, J = 409, 12, 1H, PH), 3.42 (broad, 3H, *o*-Me), 2.54 (broad, 3H, *o*-Me), 2.26 (6H, *p*-Me), 1.87 (broad, 3H, *o*-Me), 1.26 (broad, 3H, *o*-Me). ^{1}H NMR (CD_2Cl_2, −20 °C): δ 7.61 (broad, 6H, Ph), 7.48–7.46 (m, 3H, Ph), 7.35–7.32 (m, 6H, Ph), 6.92 (1H, Mes), 6.86 (1H, Mes), 6.75 (1H, Mes), 6.63 (1H, Mes), 4.82 (dd, J = 414, 13, 1H, PH), 3.38 (3H, *o*-Me), 2.50 (3H, *o*-Me), 2.25 (3H, *p*-Me), 2.23 (3H, *p*-Me), 1.85 (3H, *o*-Me), 1.20 (3H, *o*-Me). IR: 3436, 3025, 2919, 2731, 2413, 1601, 1431, 1378, 1096, 1025, 943, 902, 849, 743, 690, 620, 532.

4.12. *cis*-Pt(PMes$_2$H)$_2$(Me)(Cl) (**6**)

A light brown solution of Pt(cod)(Me)(Cl) (100 mg, 0.283 mmol) in CH_2Cl_2 (6 ml) was treated with $PMes_2H$ (153 mg, 0.565 mmol). Petroleum ether (11 ml) was layered on the solution and the mixture was cooled to −20 °C to give 109 mg (49%) of white crystals in two crops.

Anal. Calc. for $C_{37}H_{49}ClP_2Pt$: C, 56.52; H, 6.28. Found: C, 56.43; H, 6.25%. ^{31}P{^{1}H} NMR (CD_2Cl_2, 21 °C): δ −33.9 (J_{Pt-P} = 1492), −45.1 (J_{Pt-P} = 4344). ^{1}H NMR (CD_2Cl_2, 21 °C): δ 6.74 (broad, Mes), 2.34 (broad, *o*-Me), 2.23 (*p*-Me), 0.60 (m, J_{Pt-P} = 50, Pt–Me). ^{1}H NMR (CD_2Cl_2, −70 °C): δ 6.97–6.79 (m, Mes), 6.72–6.67 (m, Mes), 6.59–6.58 (m, Mes), 6.51–6.48 (m, Mes), 6.42 (Mes), 6.37 (apparent dd, J = 449, 5, 1H, PH), 6.10–6.08 (m), 6.03 (Mes), 6.00 (Mes), 5.71 (d, J = 434, 1H, PH), 5.26 (apparent dd, J = 403, 17, 1H, PH), 5.13 (apparent dd, J = 360, 5, 1H, PH), 4.56 (apparent dd, J = 366, 7, 1H, PH), 3.26–3.20 (m, Me), 3.16 (Me), 3.00 (Me), 2.65–2.58 (m, Me), 2.52 (Me), 2.38 (Me), 2.22–2.18 (m, Me), 2.06–2.01 (m, Me), 1.95–1.93 (m, Me), 1.77 (Me), 1.66 (Me), 1.52 (Me), 1.47 (Me), 1.30 (Me), 0.86 (Me), 0.51–0.37 (Pt–Me). ^{13}C{^{1}H} NMR (CD_2Cl_2, 21 °C): δ 142.7 (m), 142.4 (very broad), 140.8 (Mes), 140.6 (Mes), 140.0 (Mes), 130.2 (m, Mes), 123.5 (broad), 122.5, 121.5 (broad), 23.6–22.5 (very broad), 23.1 (m, *o*-Me), 21.1 (*p*-Me), 21.0 (*p*-Me), 3.5 (dd, J = 96, 6, Pt–Me). IR: 3444, 2955, 2911, 2722, 2400, 1600, 1555, 1444, 1405, 1377, 1255, 1200, 1027, 944, 900, 850, 805, 700, 611, 550, 461.

4.13. *cis*-Pt(PMes$_2$H)$_2$(Et)(I) (**7**)

Pt(cod)(Et)(I) (418 mg, 0.910 mmol) was dissolved in methylene chloride (5 ml). $PMes_2H$ (492 mg, 1.82 mmol) was added. Petroleum ether (3 ml) was layered on top of the yellow solution. The solution was refrigerated at 3 °C to give off-white crystals (480 mg, 60%, in two crops).

Anal. Calc. for $C_{38}H_{51}IP_2Pt$: C, 51.18; H, 5.76. Found: C, 51.07; H, 5.85%. ^{1}H NMR ($CDCl_3$): δ 6.71 (broad, 8H, Mes), 2.23 (broad m, 36H, Me), 1.07 (broad, 5H, Et). The PH peaks were not observed. ^{13}C{^{1}H} NMR ($CDCl_3$): δ 143.0 (very broad, Mes), 140.9 (Mes), 140.7 (Mes), 140.0 (Mes), 130.4 (broad m, Mes), 125.4 (Mes), 124.9 (Mes), 121.5 (Mes), 24.1–22.6 (very broad, *o*-Me), 21.8 (*p*-Me), 21.7 (*p*-Me), 21.6 (*p*-Me), 18.8 (CH_2CH_3), 10.4 (d, J = 93, CH_2CH_3). IR: 2915, 2844, 2402, 1603, 1556, 1447, 1407, 1374, 1292, 1263, 1186, 1030, 946, 905, 848, 734, 612, 572, 552, 506, 457, 426, 408. ^{1}H NMR (CD_2Cl_2, 21 °C): δ 6.77 (broad, 8H, Mes) 2.6–2.0 (broad m, *o*-Me), 2.22 (*p*-Me), 1.02 (broad, 5H, Et). The PH signals were not observed. ^{31}P{^{1}H} NMR (CD_2Cl_2, 21 °C): δ −39.9 (very broad, $J_{Pt-P} \approx 4500$) −43.5 (very broad, $J_{Pt-P} \approx 1310$).

^{1}H NMR (CD_2Cl_2, −60 °C): Six different PH groups were observed, confirmed by ^{1}H{^{31}P} NMR: δ 6.82 (obscured by Mes, d, J = 353, 1H, PH), 6.75 (obscured by Mes, d, J = 324, 1H, PH), 5.86 (apparent dd, J = 395, 16, 1H, PH), 5.41 (apparent dd, J = 400, 17, 1H, PH), 5.18 (apparent dd, J = 354, 6, 1H, PH), 4.71 (apparent dd, J = 361, 8, 1H, PH). Additional signals: δ 6.95–6.88 (m, Mes), 6.81–6.79 (m, Mes), 6.69–6.67 (m, Mes), 6.57 (Mes), 6.46 (Mes), 6.35–6.32 (m, Mes), 6.02–5.99 (m, Mes), 3.18–3.17 (m, Me), 3.12–3.11 (m, Me), 3.01 (Me), 2.89 (Me), 2.64 (Me), 2.59 (Me), 2.54 (Me), 2.50 (Me), 2.32–2.27 (m, Me), 2.23–2.18 (broad m, Me), 2.08–2.01 (broad m, Me), 1.99 (Me), 1.91 (Me), 1.88 (Me), 1.85 (Me), 1.80 (Me), 1.76 (Me), 1.66 (Me), 1.50–1.48 (m, Me), 1.33–1.26 (m, Me), 1.16–1.12 (m, Me), 0.94 (Me), 0.83 (Me), 0.71–0.66 (m, Pt–Et), 0.59–0.54 (m, Pt–Et).

4.14. *trans*-Pt(PMes$_2$H)$_2$(Et)(I) (**8**)

cis-PtL_2(Et)(I) (91 mg, 0.10 mmol) was dissolved in approximately 1 ml of $CDCl_3$ to give a yellow solution, which was heated for 4 days at 40 °C and monitored by ^{1}H NMR. When the isomerization to the *trans* compound was complete, the contents of the NMR tube were poured into a vial and petroleum ether was layered

on top. After 3 days, 72 mg (80%) of a bright yellow precipitate formed. Recrystallization from CH_2Cl_2/ether gave analytically pure light yellow crystals.

Anal. Calc. for $C_{38}H_{51}IP_2Pt$: C, 51.18; H, 5.76. Found: C, 50.81; H, 5.80. $^{31}P\{^1H\}$ NMR ($CDCl_3$): δ −39.5 (broad, J_{Pt-P} = ca. 3350). ^1H NMR ($CDCl_3$): δ 6.88 (8H, Mes), 2.48 (broad, Me), 2.30 (broad, Me), 1.10 (q, $J_{H-H}=7$, $J_{Pt-H}=114$, 2H, CH_2CH_3), 0.68 (t, $J_{H-H}=7$, $J_{Pt-H}=70$, 3H, CH_2CH_3). The PH peaks were not observed. $^{13}C\{^1H\}$ NMR (CD_2Cl_2): δ 143.1 (Mes), 140.9 (Mes), 130.6 (Mes), 124.1 (broad, Mes), 23.8 (broad, *o*-Me), 21.5 (*p*-Me), 17.6 (CH_2CH_3), 6.0 ($J_{Pt-C}=671$, CH_2CH_3). IR: 3440, 2953, 2906, 2846, 2728, 2395, 1604, 1556, 1443, 1408, 1378, 1289, 1259, 1200, 1063, 1028, 850, 802, 612, 553, 422.

^1H NMR (CD_2Cl_2, 21 °C): δ 6.96 (8H, Mes), 2.51 (24H, *o*-Mes), 2.42 (12H, *p*-Mes), 1.16 (q, $J_{H-H}=7$, $J_{Pt-H}=83$, CH_2CH_3), 0.73 (t, $J_{H-H}=7$, $J_{Pt-H}=70$, CH_2CH_3). $^{31}P\{^1H\}$ NMR (CD_2Cl_2, 21 °C): δ −39.0 ($J_{Pt-P}=3099$). ^1H NMR (CD_2Cl_2, −70 °C): The four expected PH signals were observed by ^1H and $^1H\{^{31}P\}$ NMR, but their low intensity and the presence of Mes signals precluded detailed analysis of the AA′XX′ patterns. Instead we report the separation between the two most intense lines of these patterns for a given resonance. δ 7.35 (apparent d, J = ca. 400), 7.1 (obscured by Mes), 6.8 (apparent d, $J=355$), 6.15 (apparent d, $J=375$). Additional signals: δ 7.15–6.70 (broad m, Mes), 3.23 (Me), 3.22 (Me), 3.17 (Me), 3.03 (Me), 2.62 (Me), 2.34 (Me), 2.29 (Me), 2.27 (Me), 2.08 (Me), 2.04 (Me), 1.87 (Me), 1.75 (Me), 1.67 (Me), 1.51 (Me), 1.50 (Me), 1.16–1.11 (m, Me), 0.89–0.87 (m, Me), 0.80–0.60 (broad m, Me), 0.45 (m, Pt–Et), 0.29 (m, Pt–Et).

^1H NMR (C_6D_5Cl, 21 °C): δ 6.72 (Mes), 2.52 (*o*-Me), 2.07 (p-Me), 1.35 (m, Pt–Et), 0.84 (m, Pt–Et). The PH resonances were not observed. $^{31}P\{^1H\}$ NMR (C_6D_5Cl, 21 °C): δ −36.8 (very broad, J_{Pt-P} = ca. 3300). ^1H NMR (C_6D_5Cl, 80 °C): δ 7.24 (apparent d, $J=384$, $J_{Pt-H}=26$, perhaps the most intense two peaks of an AA′XX′ pattern), 6.72 (Mes), 2.51 (*o*-Me), 2.08 (*p*-Me), 1.33 (q, $J_{HH}=8$, $J_{Pt-H}=84$, CH_2CH_3), 0.84 (t, $J_{HH}=8$, $J_{Pt-H}=72$, CH_2CH_3).

4.15. $PMes_2H\cdot BH_3$ (**9**)

A clear solution of $PMes_2H$ (300 mg, 1.11 mmol) in THF (6 ml) was cooled to 0 °C and treated with 834 μl of $BH_3\cdot SMe_2$ (1.67 mmol). The solution was warmed to room temperature with stirring. The solvent was removed under vacuum to give a white solid, which was recrystallized from petroleum ether at 0 °C to give large white crystals (297 mg, 95%, in four crops). *Anal.* Calc. for $C_{18}H_{26}BP$: C, 76.08; H, 9.22. Found: C, 75.73; H, 9.37%. $^{31}P\{^1H\}$ NMR (C_6D_6): δ −27.3 (broad). ^{31}P NMR (C_6D_6): δ −27.3 (broad d, $J_{PH}=383$). ^1H NMR (C_6D_6): δ 6.53 (d, $J=3$, 4H, Mes), 6.42 (dq, $J=382$, 8, PH), 2.29 (12H, *o*-Me), 1.96 (6H, *p*-Me). The BH_3 protons were not observed. $^{13}C\{^1H\}$ NMR (C_6D_6): δ 143.0 (d, $J=9$, Mes), 141.1 (d, $J=2$, Mes), 130.8 (d, $J=8$, Mes), 123.4 (d, $J=50$, Mes), 22.3 (d, $J=6$, *o*-Me), 21.2 (*p*-Me). IR: 3445, 3026, 2952, 2732, 2406, 2376, 2338, 2255, 2115, 1725, 1633, 1602, 1446, 1384, 1135, 1061, 1030, 967, 943, 893, 849, 756, 694, 626, 545.

4.16. Crystallographic structural determination

Crystal, data collection, and refinement parameters are given in Table 3. A Siemens P4 diffractometer equipped with a CCD detector was used. The structures were solved using direct methods, completed by subsequent difference Fourier syntheses and refined by full-matrix least-squares procedures. All non-hydrogen atoms were refined anisotropically. The P–H hydrogens were located from the electron difference map and allowed to refine isotropically. All software and sources of the scattering factors are contained in the SHELXTL (5.10) program library (G. Sheldrick, Siemens XRD, Madison, WI). The figures were prepared using either SHELXTL or ORTEP-3 for Windows [31].

4.17. Cone angle calculations

Cone angles were calculated using the program STERIC [21], as previously reported [32]. Hydrogen atoms, as placed in the crystallographic determination, were fixed at a C–H distance of 1.1 Å, and a P–H distance of 1.42 Å [33]. Calculations on **5**·$2CH_2Cl_2$ showed that changing the P–H distance from 1.22 to 1.50 Å had minimal effect (change from 147° to 149°) on the cone angle. The M–P bond distances were fixed at 2.28 Å [22]. The CPK van der Waals radii set was used for all cone angle calculations.

5. Supplementary material

Crystallographic data for the structures reported in this paper have been deposited with the Cambridge Crystallographic Data Centre, CCDC Nos. 181084–181086 and 181088–181089. Copies of this information may be obtained free of charge from The Director, CCDC, 12 Union Road, Cambridge, CB2 1EZ, UK (fax: +44-1223-336033; e-mail: deposit@ccdc.cam.ac.uk or www: http://www.ccdc.cam.ac.uk).

Acknowledgements

We thank the NSF Career Program, DuPont, and Union Carbide (Innovation Recognition Award) for support, and the Department of Education for a GAANN fellowship for M.A.Z. The University of

Delaware acknowledges the NSF (Grant CHE-9628768) for their support of the purchase of the CCD-based diffractometer.

References

[1] W. Levason, in: F.R. Hartley (Ed.), The Chemistry of Organophosphorus Compounds, vol. 1, Wiley, Chichester, England, 1990, pp. 567–641.
[2] For selected examples of secondary phosphine complexes, see: (a) C. Masters, B.L. Shaw, J. Chem. Soc. (A) (1971) 3679; (b) P. Leoni, Organometallics 12 (1993) 2432; (c) H.-C. Bottcher, M. Graf, K. Merzweiler, Polyhedron 16 (1997) 341; (d) R.G. Hayter, J. Am. Chem. Soc. 84 (1962) 3046; (e) R.J. Forder, I.S. Mitchell, G. Reid, R.H. Simpson, Polyhedron 13 (1994) 2129; (f) R. Giannandrea, P. Mastrorilli, C.F. Nobile, Inorg. Chim. Acta 284 (1999) 116; (g) T. Campbell, A.M. Gibson, R. Hart, S.D. Orchard, S.J.A. Pope, G. Reid, J. Organomet. Chem. 592 (1999) 296; (h) M.L. Buil, M.A. Esteruelas, E. Onate, N. Ruiz, Organometallics 17 (1998) 3346; (i) P. Leoni, G. Chiaradonna, M. Pasquali, F. Marchetti, A. Fortunelli, G. Germano, Inorg. Chim. Acta 264 (1997) 185; (j) A. Albinati, F. Lianza, M. Pasquali, M. Sommovigo, P. Leoni, P.S. Pregosin, H. Ruegger, Inorg. Chem. 30 (1991) 4690.
[3] I.V. Kourkine, M.D. Sargent, D.S. Glueck, Organometallics 17 (1998) 125.
[4] M.A. Zhuravel, N.S. Grewal, D.S. Glueck, K.-C. Lam, A.L. Rheingold, Organometallics 19 (2000) 2882.
[5] For complementary studies of mesitylphosphine ($PMesH_2$), see: I.V. Kourkine, S.V. Maslennikov, R. Ditchfield, D.S. Glueck, G.P.A. Yap, L.M. Liable-Sands, A.L. Rheingold, Inorg. Chem. 35 (1996) 6708.
[6] W. de Graaf, J. Boersma, W.J.J. Smeets, A.L. Spek, G. van Koten, Organometallics 8 (1989) 2907.
[7] R.K. Harris, Can. J. Chem. 42 (1964) 2275.
[8] (a) A. Gillie, J.K. Stille, J. Am. Chem. Soc. 102 (1980) 4933; (b) J. Krause, G. Cestaric, K.-J. Haack, K. Seevogel, W. Storm, K.-R. Pörschke, J. Am. Chem. Soc. 121 (1999) 9807.
[9] F.R. Hartley, The Chemistry of Platinum and Palladium, Wiley, New York, 1973.
[10] P. Budzelaar, gNMR, V3.6.5, Cherwell Scientific Publishing, Oxford, 1996.
[11] P.S. Pregosin, R.W. Kunz, ^{31}P and ^{13}C NMR of Transition Metal Phosphine Complexes, Springer-Verlag, New York, 1979.
[12] R.G. Pearson, Inorg. Chem. 12 (1973) 712.
[13] J. Vicente, A. Arcas, D. Bautista, P.G. Jones, Organometallics 16 (1997) 2127.
[14] S.H. Mastin, P. Haake, J. Chem. Soc., Chem. Commun. (1970) 202.
[15] G.K. Anderson, J.A. Davies, D.J. Schoeck, Inorg. Chim. Acta 76 (1983) L251.
[16] A.G. Orpen, L. Brammer, F.H. Allen, O. Kennard, D.G. Watson, R. Taylor, J. Chem. Soc., Dalton Trans. (1989) S1.
[17] G.K. Anderson, H.C. Clark, J.A. Davies, G. Ferguson, M. Parvez, J. Cryst. Spectr. Res. 12 (1982) 449.
[18] F.R. Hartley, Chem. Soc. Rev. 2 (1973) 163.
[19] J.M. Brunel, B. Faure, M. Maffei, Coord. Chem. Rev. 178–180 (1998) 665.
[20] R.A. Bartlett, M.M. Olmstead, P.P. Power, G.A. Sigel, Inorg. Chem. 26 (1987) 1941.
[21] (a) B.C. Taverner, J. Comput. Chem. 17 (1996) 1612; (b) B.C. Taverner, STERIC 1.12B, 1997. Available on the Internet at http://www.gh.wits.ac.za.
[22] C.A. Tolman, Chem. Rev. 77 (1977) 313.
[23] (a) A. Bright, B.E. Mann, C. Masters, B.L. Shaw, R.M. Slade, R.E. Stainbank, J. Chem. Soc. (A) (1971) 1826; (b) R. Giannandrea, P. Mastrorilli, M. Palma, F.P. Fanizzi, U. Englert, C.F. Nobile, Eur. J. Inorg. Chem. (2000) 2573.
[24] C.H. Bushweller, C.D. Rithner, D.J. Butcher, Inorg. Chem. 25 (1986) 1610.
[25] A.B. Pangborn, M.A. Giardello, R.H. Grubbs, R.K. Rosen, F.J. Timmers, Organometallics 15 (1996) 1518.
[26] D. Drew, J.R. Doyle, Inorg. Synth. 28 (1990) 346.
[27] G.K. Anderson, M. Lin, Inorg. Synth. 28 (1990) 60.
[28] J.X. McDermott, J.F. White, G.M. Whitesides, J. Am. Chem. Soc. 98 (1976) 6521.
[29] H.C. Clark, L.E. Manzer, J. Organomet. Chem. 59 (1973) 411.
[30] T.G. Appleton, M.A. Bennett, Inorg. Chem. 17 (1978) 738.
[31] L.J. Farrugia, J. Appl. Cryst. 30 (1997) 565.
[32] J.M. Smith, N.J. Coville, L.M. Cook, J.C.A. Boeyens, Organometallics 19 (2000) 5273.
[33] CRC Handbook of Chemistry and Physics, 71st ed., CRC Press, Boca Raton, FL, 1990.